The Journal of Experimental Biology 204, 1421–1431 (2001)
Printed in Great Britain © The Company of Biologists Limited 2001
JEB3222

SCALE EFFECTS ON THE ATTACHMENT PADS AND FRICTION FORCES IN SYRPHID FLIES (DIPTERA, SYRPHIDAE)

STANISLAV GORB*, ELENA GORB AND VICTORIA KASTNER

Biological Microtribology Group, Biochemistry Department, Max-Planck-Institute of Developmental Biology, Spemannstrasse 35, D-72076 Tübingen, Germany

*e-mail: Stas.Gorb@tuebingen.mpg.de

Accepted 24 January; published on WWW 28 March 2001

Summary

To test the role of constructional and dimensional factors in the generation of friction force by systems of setose attachment pads, six species of syrphid fly (*Platycheirus angustatus*, *Sphaerophoria scripta*, *Episyrphus balteatus*, *Eristalis tenax*, *Myathropa florea* and *Volucella pellucens*) were studied using light and scanning electron microscopy. Flies were selected according to their various body mass and attachment pad dimensions. Such variables as pad area, setal density, the area of a single setal tip and body mass were individually measured. A centrifugal force tester, equipped with a fibre-optic sensor, was used to measure the friction forces of the pads on a smooth horizontal surface made of polyvinylchloride. Friction force, which is the resistance force of the insect mass against the sum of centrifugal and tangential forces, was greater in heavier insects such as *Er. tenax*, *M. florea* and *V. pellucens*. Although lighter species generated lower frictional forces, the acceleration required to detach an insect was greater in smaller species. The area of attachment pads, setal tip area and setal density differed significantly in the species studied, and the dependence of these variables on body mass was significant.

The frictional properties of the material of the setal tips were not dependent on the dimensions of the fly species. Similar results were obtained for the frictional properties of the pulvillus as a whole. Thus, the properties of the secretion and the mechanical properties of the material of the setal tips are approximately constant among the species studied. It is concluded that differences in friction force must be related mainly to variations in the real contact area generated by the pad on the smooth surface. The real contact area can be estimated as the summed area of the broadened setal tips of the pad in contact with the surface. The real contact area depends on such morphological variables as setal density and the area of a single setal tip. Although individual variables vary among flies with different dimensions, they usually compensate such that smaller setal tip area is partially compensated for by higher setal density.

Key words: morphology, cuticle, material properties, scale effect, friction, attachment, Insecta, Diptera, syrphid fly.

Introduction

During their evolution, insects have evolved two distinctly different mechanisms to attach themselves to a variety of substrata: smooth flexible pads and setose surfaces. Attachment forces mediated by friction or adhesion are usually proportional to the area of real contact between two surfaces (Persson, 1998). Because of the flexible material of the pads, both mechanisms can maximise the possible real contact area with the substratum, regardless of its microsculpture. Setose systems always contain cuticle protuberances in their surfaces. The protuberances occurring on the setose pads of Coleoptera (Stork, 1980a; Stork, 1980b), Dermaptera (Beutel and Gorb, 2000) and Diptera (Bauchhenss, 1979; Bauchhenss and Renner, 1977; Gorb, 1998b) belong to different types. Representatives of the first two lineages have setae, 5–50 μm long, with sockets on the ventral surface of their tarsal segments. Dipteran protuberances are acanthae, protuberances originating from a single cell and lacking sockets (Richards and Richards, 1969).

Data on the setose pad system of an adult reduviid bug (*Rhodnius prolixus*) led previous authors to suggest that mechanical interlocking between adhesive setae and irregularities in the substratum is responsible for attachment to the substratum (Gillett and Wigglesworth, 1932). Most authors agree that at least two factors related to the pad material can contribute to the attachment force: (i) material flexibility and (ii) the presence of an epidermal secretion in the contact area. The deformability and visco-elastic properties of smooth pads have been suggested to be important (Brainerd, 1994), and this was recently confirmed experimentally (Jiao et al., 2000; Gorb et al., 2000). It has been shown that the adhesive secretion is an essential component of attachment in both setose and smooth systems. Pad fluids have been found on the smooth pads of cockroaches (Roth and Willis, 1952), aphids (Lees and Hardie, 1988; Dixon et al., 1990) and bugs (Hasenfuss, 1977; Hasenfuss, 1978; Ghasi-Bayat and Hasenfuss, 1980) and on the

setose adhesive pads of reduviid bugs (Edwards and Tarkanian, 1970), flies (Bauchhenss and Renner, 1977; Bauchhenss, 1979; Walker et al., 1985) and coccinellid beetles (Ishii, 1987).

Although the morphology and ultrastructure of the setose attachment devices have been described in numerous studies, various aspects of the functioning of these systems still remain unclear. Among lizards, which are also able to walk on a smooth surface using 'setose pads', the pad area has been shown to be the primary factor influencing clinging ability in geckos, skinks and iguanids (Irschick et al., 1996). However, despite the close correlation between pad area and attachment ability, pad area depends on body mass less than does attachment ability. When the effect of body size is removed, approximately 50 % of the variation in clinging ability remains unexplained, which suggests that microsculptural and ultrastructural differences may affect clinging ability. Geckos, skinks and iguanids differ in the structure of the setae covering the attachment pads (Ruibal and Ernst, 1965; Ernst and Ruibal, 1967). However, the effect of ultrastructural properties has not been investigated systematically.

In the beetle *Chrysolina polita*, attachment force increases with the total number of adhesive setae (Stork, 1980b). The number of adhesive setae can contribute to the attachment force by increasing the number of single contact points and/or by increasing the overall contact area with the substratum. To test the role of constructional and dimensional factors in attachment, a larger number of species must be tested. Such variables as pad area, setal density, the area of a single setal tip and body mass must be individually measured to investigate their effects on the resulting attachment force. Previously, measurements of attachment forces in living insects have been confounded by difficulties in experimental design or by the time-consuming processing of video recordings. In this study, we improved the previously used centrifugal method of measuring attachment force by incorporating a laser beam system and fibre-optic sensor to monitor the position of the insect on a drum. This method was used to test individual attachment performance in six species of syrphid fly, chosen according to their body mass and attachment pad dimensions. The variety of attachment pad design in a number of taxa of the family Syrphidae has been described previously (Röder, 1984). In our study, most morphological data were collected individually, allowing us to compare directly the effects of structural properties on attachment ability. Lateral attachment force, to which friction force is the main contributor, was measured.

Materials and methods

Animals

Male flies of six common species from the family Syrphidae were captured in July 1999 in the Schönbuch forest (near Tübingen, southwest Germany): *Platycheirus angustatus* (Z.), *Sphaerophoria scripta* (L.), *Episyrphus balteatus* (De Geer), *Eristalis tenax* (L.), *Myathropa florea* (L.) and *Volucella pellucens* (L.). After capture, the wings were carefully cut off without anaesthesia. Anaesthesia was not used because, without a recovery period, it may disturb the normal posture of animals and, thus, influence attachment ability. To minimise water loss through the cut wing bases, experiments were carried out 5–15 min after wing excision. After the experiments, the insects were labelled and placed in 70 % ethanol for processing for microscopy.

Force measurements

A centrifugal technique was used. The main advantage of this method, especially in the case of small organisms, is that no prior treatment of the insects is required. This method is commonly used for the measurement of friction and adhesive forces for a variety of objects. It has been applied to measure the adhesion strength between starch microspheres and microcrystalline cellulose (Podczeck and Newton, 1995), the frictional properties of skin (Highley et al., 1977), the strength of barnacle cement (Dougherty, 1990) and insect attachment forces (Dixon et al., 1990; Brainerd, 1994; Federle et al., 2000).

Our equipment was improved to enable such variables as initial motor speed and motor acceleration to be varied and to acquire, automatically, data on motor speed and insect position relative to the rotor centre (Fig. 1). The motor rotating the drum was controlled by a computer. Just above the drum, a laser beam, serving as a light source, and a fibre-optic sensor were mounted. The sensitivity of the fibre-optic sensor could be tuned according to the subject's dimensions. Its sensitivity was high enough to monitor subjects of approximately 1 mm in diameter rotating at 2000–2500 revs min^{-1}. The light source and the sensor were displaced by a distance (d) from the rotor centre. Given the angular speed (ω) of the motor and the time between the two interruptions of the light sensor signal (Δt_1) as an insect rotates on the disc, the radius of the position of the subject could be calculated after each rotation (Fig. 1B–D). All calculations were carried out automatically by the controlling software. The radius and other variables were displayed on the computer screen, allowing the subject's position on the drum during the experiment to be monitored directly. An insect standing on the horizontal surface of the drum covered by a smooth polyvinylchloride (PVC) plate (the contact angles of water droplet on the plate were 81–86 °) was accelerated until it lost contact with the drum. When the insect left the drum surface, the sensor no longer received a signal from the subject, and the motor acceleration was automatically interrupted, the experiment stopped and data saved. The following variables were measured: sensor displacement from the rotor centre d (cm), motor speed v (revs min^{-1}), mass m (mg), time from the beginning of rotation Δt (s) and the time between two sensor signals Δt_1 (s). In addition, the following variables were calculated. The angular speed ω (rad s^{-1}) was calculated as:

$$\omega = \frac{1}{30}\pi\nu . \quad (1)$$

The angular speed was used to calculate the radius of rotation r (cm):

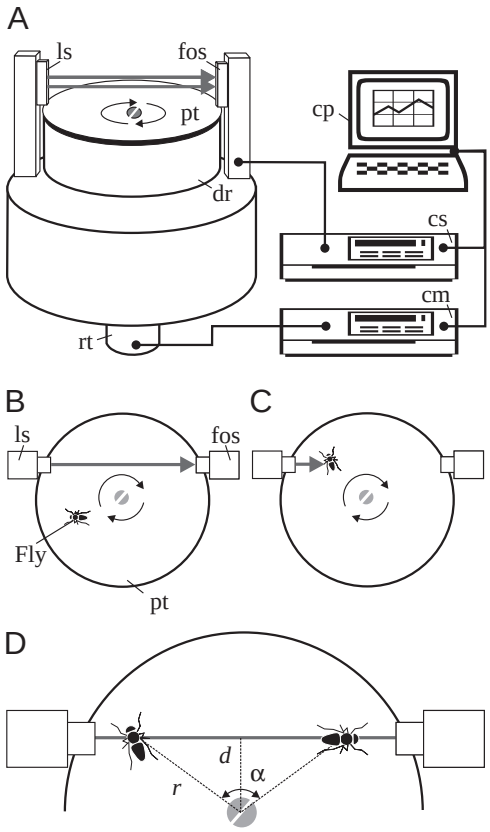

Fig. 1. Centrifugal device for measuring frictional force. (A) Layout of the centrifuge. The metal drum (dr), covered by a polyvinyl-chloride disc (pt), is driven by the computer-controlled motor. The fibre-optic sensor (fos) is adjusted to be just above the disc. The sensor signal is monitored by a computer (cp). (B–D) Diagrams showing the technique used to monitor insect position (view onto the disc surface from above). The sensor is shifted to one side of the disc by a distance *d* from its centre. The fly, rotating clockwise, passes the laser beam twice per rotation, thus interrupting the sensor signal twice. Given the speed of the motor and the time between signal interruptions, the position of the fly on the disc can be calculated (D). α, angle between detected fly positions and the drum centre; cs, sensor control electronics; cm, motor control electronics; *d*, displacement of the sensor from the drum centre; ls, light source; *r*, radius of the position of the fly from the rotor centre; rt, rotor of the motor.

$$r = d\cos\left(\frac{\omega}{2\Delta t_1}\right), \tag{2}$$

the centrifugal component of the acceleration a_c ($m\,s^{-2}$):

$$a_c = \frac{1}{100} r\omega^2, \tag{3}$$

and the tangential component of the acceleration a_t ($m\,s^2$):

$$a_t = \frac{\Delta\omega r}{100\Delta t}. \tag{4}$$

Knowing a_c, the centrifugal component of the friction force F_c (mN) was calculated:

$$F_c = \frac{1}{1000} m a_c. \tag{5}$$

Knowing a_t, the tangential component of the friction force F_t (mN) was calculated:

$$F_t = \frac{1}{1000} m a_t. \tag{6}$$

The total friction force F (mN) was obtained from the centrifugal F_c and tangential F_t components of the friction force:

$$F = \sqrt{F_c^2 + F_t^2}, \tag{7}$$

and the total acceleration a ($m\,s^{-2}$) was obtained from the centrifugal a_c and tangential a_t components of the acceleration:

$$a = \sqrt{a_c^2 + a_t^2}. \tag{8}$$

Prior to force measurements, an individual insect was weighed using a Mettler Toledo AG204 balance with a precision of 0.1 mg. The number of individual flies (*N*) and number of tests (*n*) for each species was as follows: *Platycheirus angustatus* (*N*=6, *n*=60), *Sphaerophoria scripta* (*N*=4, *n*=40), *Episyrphus balteatus* (*N*=11, *n*=110), *Eristalis tenax* (*N*=9, *n*=90), *Myathropa florea* (*N*=3, *n*=30) and *Volucella pellucens* (*N*=5, *n*=50). Ten repetitions of force measurements were made for each individual fly. No statistically significant differences were revealed in fly performance depending on the number of experiments. For example, the relationship between friction force and experiment number was estimated for *Er. tenax* (*N*=8, *n*=10 tests for each insect, Kruskal–Wallis one-way analysis of variance, ANOVA, on ranks, H=7.634, d.f.=9, P=0.571). Similar results have been reported for ants (Federle et al., 2000).

We made corresponding calculations to evaluate possible drag F_{drag} for each experiment (*n*=371):

$$F_{drag} = \frac{1}{2} CArv^2, \tag{9}$$

where C is the empirical drag coefficient (usually approximately 1, dimensionless), A is the area of the object in a plane perpendicular to the object's motion, r is the density of the medium (r_{air}=1.29 $kg\,m^{-3}$) and v is the linear speed.

Since we did not know the orientation of the insect on the drum, we assumed that the insect always stood parallel to the drum radius and that the insect's area, in a plane perpendicular to the object's motion, was the maximum possible. These data were obtained from digitised video frames for all six species. The maximum linear speed of the insect was calculated from the maximum rotational speed, which was recorded during each experiment. Calculated average drag was 0.056 mN (*P. angustatus*, 3.5 % of the average friction force), 0.110 mN (*S. scripta*, 1.28 %), 0.200 mN (*Ep. balteatus*, 0.88 %), 0.404 mN (*Er. tenax*, 0.26 %), 0.504 mN (*M. florea*, 0.24 %) and 0.740 mN (*V. pellucens*, 0.13 %). According to these calculations, the influence of fluid flow must be minimal for such a body size and velocity.

Light microscopy

The pretarsi of flies used in force measurements were cut off the legs, dehydrated in ethanol and whole-mounted in DePeX (Serva). Each individual leg was processed separately. Digital images of pulvilli were obtained using a Sony 3CCD video camera DXC-950P mounted on a Zeiss-Axioscope light microscope. Pulvillus areas were measured from digital images using Sigma-Scan 5.0 (SPSS) software. Data were averaged separately for each individual, for each species and for each leg pair (fore-, mid- and hindlegs) within each species.

Scanning electron microscopy

Pretarsi of flies, fixed in 70 % ethanol, were dehydrated in ethanol, critical-point-dried, mounted on holders, sputter-coated with gold–palladium (10 nm) and examined in a Hitachi S-800 scanning electron microscope at 20 kV. Measurements of setal tip area and setal density per 1000 μm^2 were made from digital pictures using AnalySIS 2.1 image-analysis software (Soft-Imaging Software GmbH, Münster, Germany). The setal tip areas were measured in a total of 120–150 tenent setae from two insects for each species. The density of tenent setae was averaged for 20–60 selected pulvillar areas in each species.

Data processing

ANOVA was used to estimate differences between species according to particular variables. If the raw data were not normally distributed, Kruskal–Wallis one-way ANOVA on ranks was used. To calculate dependencies between different variables measured, linear models were applied. The ANOVA statistics (F) were also estimated for the regressions. The F-test statistic assesses the contribution of the independent variable in predicting the dependent variable. It is the ratio between the regression variation from the dependent variable mean and the residual variation about the regression line. The P-value is the probability of being wrong in concluding that there is an association between the dependent and independent variables. The smaller the P-value, the greater is the probability that there is an association. We have concluded that the independent variable could be used to predict the dependent variable when $P<0.05$.

Results

Body mass and pulvillus area

In the series of species *P. angustatus*, *S. scripta*, *Ep. balteatus*, *Er. tenax*, *M. florea* and *V. pellucens*, body mass m (mg) increased from 4.8 to 164.0 mg (Fig. 2A). Only representatives of two species (*Er. tenax* and *M. florea*) were similar in body mass. All other species differed significantly from each other (one-way ANOVA on species: $F=89.14$, $P<0.001$). Although the area of a single pulvillus S_1 (μm^2) correlates with an increased body mass (linear regression: $S_1=10\,350–286m$, $F=40.00$, $P<0.001$, one-way ANOVA), the heaviest species (*V. pellucens*) has significantly smaller pulvilli than *Er. tenax* and *M. florea* (one-way ANOVA: $F=14.29$, $P=0.001$; $F=24.48$, $P=0.001$, respectively) (Figs 2, 3).

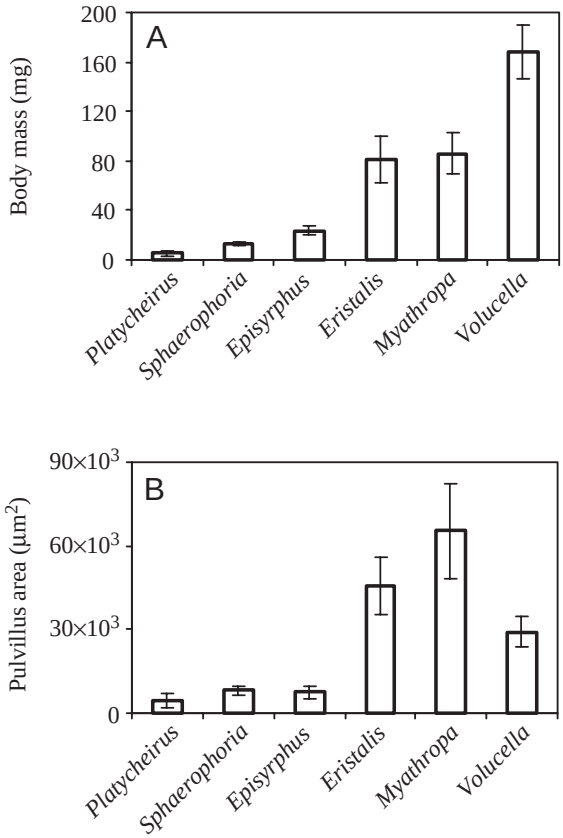

Fig. 2. Body mass (A) and area of a single pulvillus (B) for each species. Values are means ± S.D. (n=10 per species, N=3–11 depending on species, see Materials and methods).

Friction force

The acceleration at which an insect loses contact with the surface is hereafter termed ‘acceleration’. This value was significantly different among species studied (one-way ANOVA on species: $F=91.31$, $P<0.001$). The acceleration a ($m\,s^{-2}$) was greater in representatives of lighter species. It was related to the body mass m as $a=217.9–0.9m$ (linear regression: $F=7.50$, $P=0.010$, one-way ANOVA) (Figs 4A, 5A). Friction force F (mN), which is the resistance force of the insect mass to the sum of centrifugal and tangential forces, was also significantly different among species studied (one-way ANOVA on species: $F=19.32$, $P<0.001$). Friction was greater in heavier insects, such as *Er. tenax*, *M. florea* and *V. pellucens* (Figs 4B, 5B). It was related to the body mass m as $F=0.601+0.019m$ (linear regression: $F=39.34$, $P<0.001$, one-way ANOVA). Acceleration data show that, although lighter species generated lower friction forces, the ratio of friction force to the body mass is greater in smaller species. In other words, lighter species demonstrated relatively higher attachment ability.

The acceleration averaged for all trials with one species was 2–6 times lower than its maximal value for each species (Fig. 4A). A similar relationship was also obtained for friction force (Fig. 4B). The relative difference between the average measured friction force F_{ave} (mN) and the maximum measured

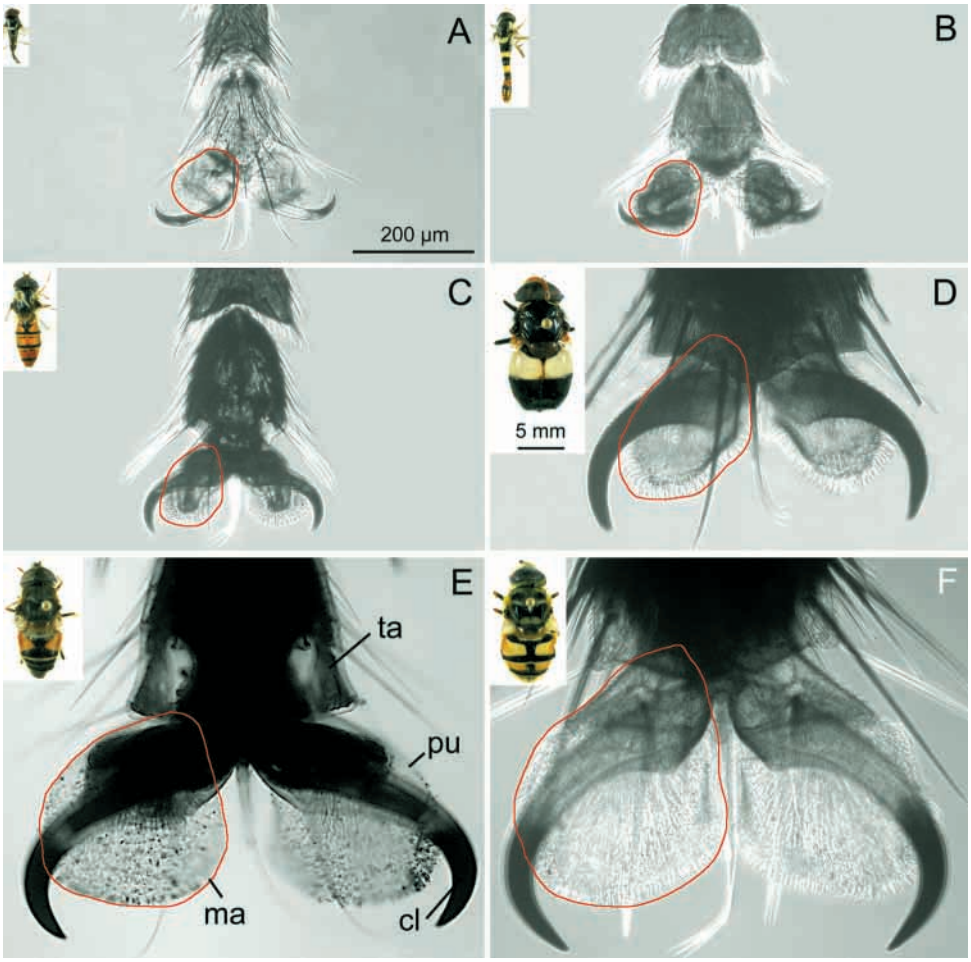

Fig. 3. Wholemounts of pretarsi of the species studied. Such preparations were used to quantify the area of a single pulvillus. Red lines indicate measured areas (ma). Insets show the species used. cl, claw; pu, pulvillus; ta, terminal tarsomere. The 200 µm scale bar applies to all micrographs, whereas the 5 mm scale bar applies to all fly insets. (A) *Platycheirus angustatus*. (B) *Sphaerophoria scripta*. (C) *Episyrphus balteatus*. (D) *Volucella pellucens*. (E) *Eristalis tenax*. (F) *Myathropa florea*.

friction force F_m (mN) was smaller in heavier insects [ΔF=64.740–0.129m, where m is mass and ΔF=100(F_{ave}/F_m); F=15.580, P<0.001, one-way ANOVA]. A similar relationship was found for the acceleration data.

Relationship between pulvillus area and friction force

There was significant relationship between body mass m and the area of a single pulvillus S_1 (linear regression: S_1=10 350–286m, F=40.00, P<0.001, one-way ANOVA) (see Fig. 7A). Since, in general, pulvillus area is larger and friction force is higher in heavier animals, it has been suggested that heavier animals generate higher friction force as a result of a larger area in contact with the substratum. The measured acceleration does not depend clearly on the pulvillus area (Fig. 6A,C), whereas the friction force increased linearly with an increase in attachment area (Figs 6B,D, 7B).

Surface characteristics of pulvilli

Given that the friction force is dependent on the area of real contact between two surfaces, it is possible that different surface characteristics of the attachment devices may contribute to differences in friction in the species studied. Two variables of the pulvillus surface were also quantified: (i) setal density and (ii) the area of the setal tip. Data obtained from scanning electron microscopy (Fig. 8) revealed significant differences in setal size and density among species (one-way ANOVA on species: setal tip area: F=489.50, P<0.001; density: F=67.55, P<0.001). Setal tip area increased and setal density slightly decreased with increased body mass. There was a significant relationship between setal tip area S_t (µm^2) or setal density D (the number of setae in 1000 µm^{-2}) and increased body mass (S_t=2.608+0.018m, F=543.30, P<0.001; D=109.1–0.331m, F=64.73, P<0.001, one-way ANOVA) (Fig. 9A,B). At the same time, setal density was correlated with setal tip area. With an increase in setal tip area, setal density decreased significantly (D=151.371–18.549S_t, F=25.51, P<0.01, one-way ANOVA) (Fig. 9C).

Lateral tenacity

Tenacity is the adhesive force per unit apparent contact area

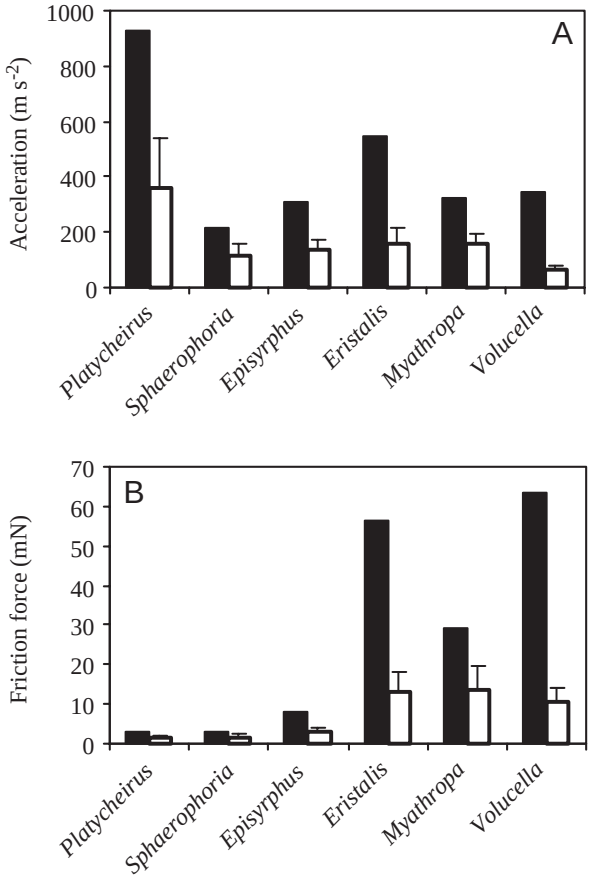

Fig. 4. Acceleration (A) and friction force (B) of the fly species. Filled columns give maximum values; open columns give means + S.D. (n=10 per species, N=3–11 depending on species, see Materials and methods).

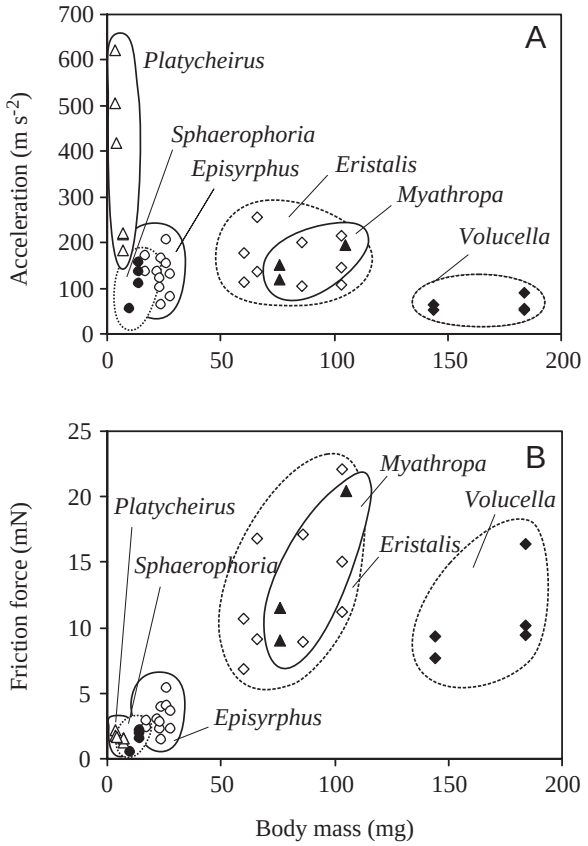

Fig. 5. Acceleration (A) and friction force (B) *versus* body mass for each specimen studied.

between two surfaces. Since, for syrphid pulvilli, friction force is mediated by adhesion, the lateral tenacity of pulvilli, τ_p ($\mu N\,\mu m^{-2}$), was calculated. This represents the friction force F per unit apparent contact area $\tau_p=F/12S_1$, where S_1 is area of a single pulvillus. The value of τ_p ranged from 0.015 to 0.035 $\mu N\,\mu m^{-2}$ in the species studied and was dependent on the body mass (Fig. 10A). However, τ_p was not dependent on pulvillus area (Fig. 10B).

However, pulvillus area is not the same as the real area of contact. The real area of contact directly influences the adhesive and frictional forces. The real contact area S_r (μm^2) was evaluated as the aggregate area of all setae on all pulvilli $S_r=12DS_1S_t$, where D is the density of tenent setae per 1 μm^2, S_1 is area of a single pulvillus in μm^2, and S_t is the area of the single setal tip in μm^2. There was no significant relationship between S_r and body mass (S_r=38.02+0.93m, F=2.36, P=0.20, one-way ANOVA) (Fig. 11A). The lateral tenacity of pulvillus material, τ_m ($\mu N\,\mu m^{-2}$), was also calculated. Since the calculated real contact area was 3–5 times smaller than the area of apparent contact (pulvillus area), τ_m was greater than τ_p. τ_m ranged from 0.06–0.13 $\mu N\,\mu m^{-2}$ in the species studied and was not dependent on body mass (τ_m=0.10–0.0002m, F=0.48, P=0.53, one-way ANOVA) (Fig. 11B).

Discussion

In a previous study, the vertical attachment forces (adhesive components) of ants measured with a centrifugal apparatus were significantly greater than those measured with a strain-gauge force transducer (Federle et al., 2000). This result has been explained by the fact that tethered insects generally continued to move during the strain-gauge measurements and only rarely were all six legs simultaneously in contact with the surface. Therefore, the centrifugal method was chosen in the present study to compare attachment abilities of syrphid flies.

Adhesion-mediated friction

In our experimental design, the horizontal force resisted by the insect during drum rotation was measured. This situation is more closely related to the situation when an insect walks on a vertical wall, and is not comparable with the situation when an insect walks under a horizontal surface because of the different directions of the forces acting on the insect. In the latter situation, the insect's weight acts in a direction more-or-less perpendicular to the surface, and adhesion is the main contributor to insect attachment. In our experimental situation, an insect resisted the force acting to move it in a direction parallel to the surface. The insect is able to resist this external force because of the friction between its attachment pads and the substratum.

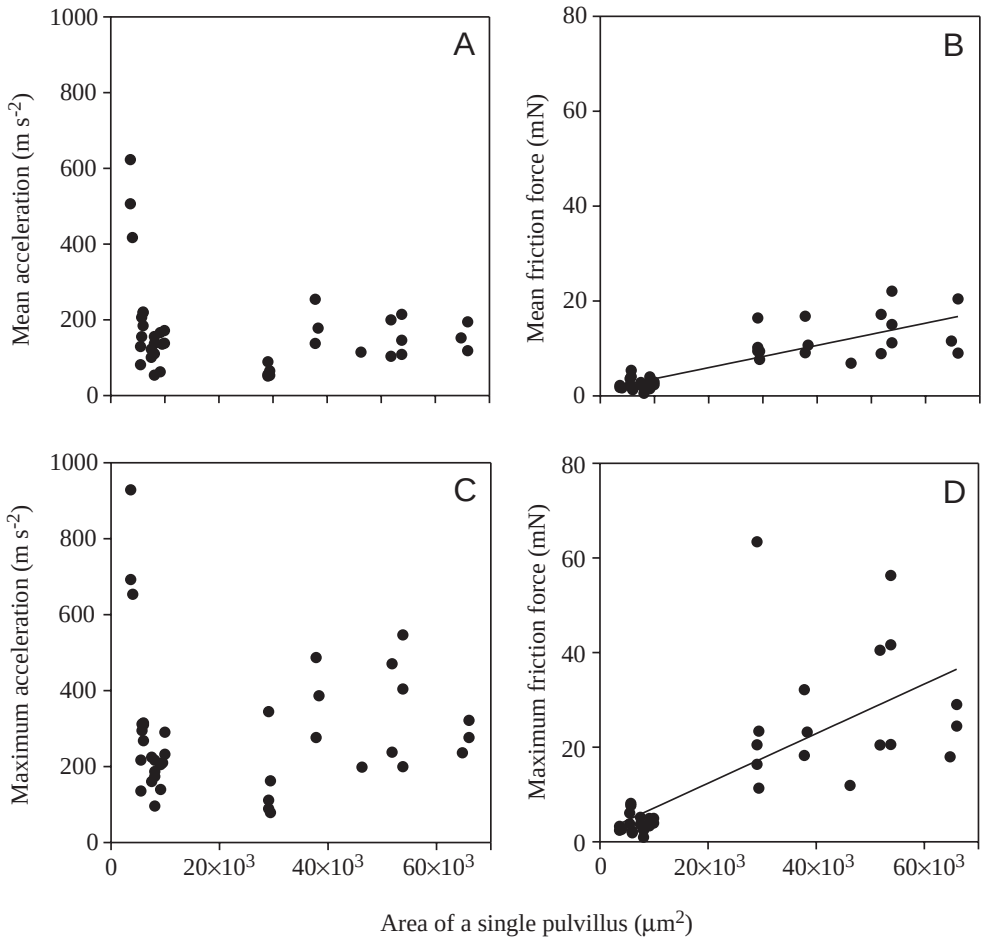

Fig. 6. Mean a_{ave} (A) and maximum a_m (C) acceleration and mean F_{ave} (B) and maximum F_m (D) friction force *versus* the area of a single pulvillus S_1 for all specimens studied. (A) Linear regression: $a_{ave}=195.7-1.21\times10^{-3}S_1$, $F=1.788$, $P=0.190$, one-way ANOVA. (B) Linear regression: $F_{ave}=1.257+2.345\times10^{-4}S_1$, $F=84.618$, $P<0.001$, one-way ANOVA. (C) Linear regression: $a_m=291.5-8.826\times10^{-6}S_1$, $F=3.987\times10^{-5}$, $P=0.995$, one-way ANOVA. (D) Linear regression: $F_m=1.892+5.241\times10^{-4}S_1$, $F=38.248$, $P<0.001$, one-way ANOVA.

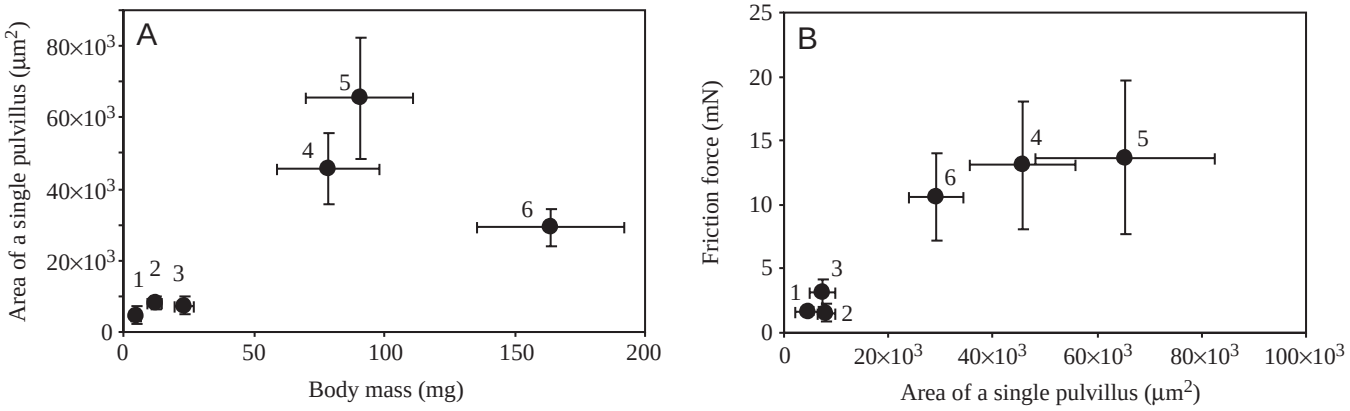

Fig. 7. Dependence of the area of a single pulvillus S_1 on body mass m (A) and of friction force F on the area of a single pulvillus (B) for the six species studied. (A) Linear regression: $S_1=10350-286m$, $F=40.00$, $P<0.001$, one-way ANOVA. (B) Linear regression: $F=1.379+2.205\times10^{-4}S_1$, $F=32.87$, $P=0.005$, one-way ANOVA. Values are means ± S.D. ($n=10$ per species, $N=3$–11 depending on species, see Materials and methods). 1, *Platycheirus angustatus*; 2, *Sphaerophoria scripta*; 3, *Episyrphus balteatus*; 4, *Eristalis tenax*; 5, *Myathropa florea*; 6, *Volucella pellucens*.

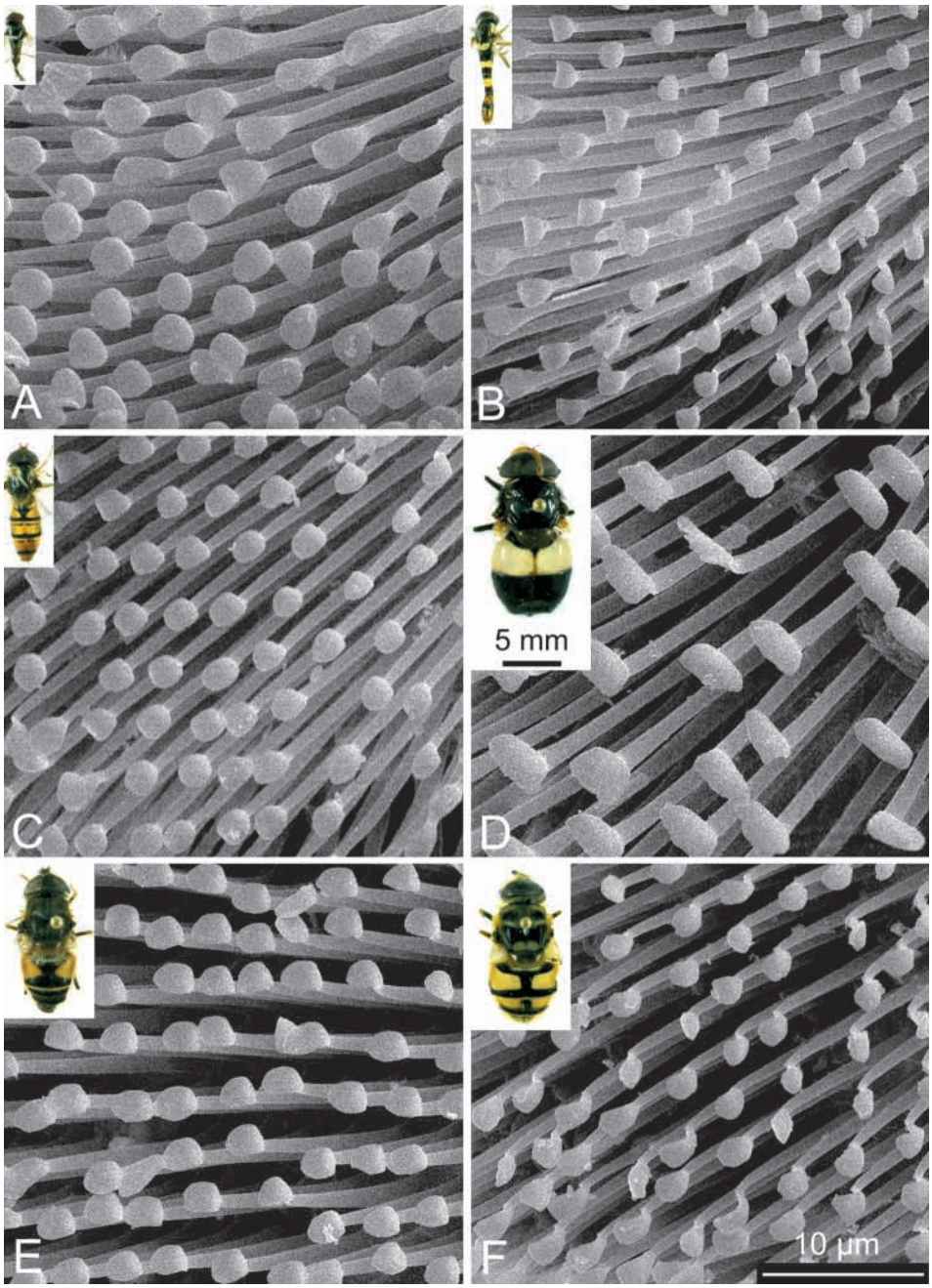

Fig. 8. Tenent setae of the species studied. Such images were used to quantify setal density and the area of the setal tip. The 10 µm scale bar applies to all micrographs, whereas the 5 mm scale bar applies to all fly insets. (A) *Platycheirus angustatus*. (B) *Sphaerophoria scripta*. (C) *Episyrphus balteatus*. (D) *Volucella pellucens*. (E) *Eristalis tenax*. (F) *Myathropa florea*.

Factors such as the proximity of two surfaces, the thickness of the fluid layer between the surfaces, surface chemistry and fluid viscosity will contribute to the adhesion force. The fine structure of the adhesive setae in syrphid flies has been reported previously for the fly *Episyrphus balteatus* (Gorb, 1998b), whose setae (acanthae) are hollow, with some containing pores under the end plate. These pores presumably allow the adhesive secretion to pass directly to the contact area. Porous canals, located at the base of the shaft, reported in other flies, are also involved in the transport of secretions to the surface (Bauchhenss, 1979). Attachment under a horizontal surface is mediated mainly by adhesive forces; these have been measured only for two insect species possessing setose attachment pads: the calliphorid fly *Calliphora vomitoria* (2.4 mN) (Walker et al., 1985) and the coccinellid beetle *Epilachna vigintioctomaculata* (2.9 mN) (Ishii, 1987). Given that the pad material is designed to deliver secretion continuously to the contact area and that adhesive forces are involved in holding an insect under a surface, we might expect that adhesive forces will contribute

to the friction force (Rabinowicz, 1995) when an insect walks on a vertical surface. Such adhesion-mediated friction can be relatively high, so that surfaces with fluid between them demonstrate a friction coefficient greater than 1. In the present study, in different species of syrphid fly, we measured friction coefficients ranging from 7 to 35, supporting a role for adhesion-mediated friction. Friction between the fly attachment system and a smooth surface is eight times greater than adhesion (Walker et al., 1985). If we assume that this relationship is similar among various fly species, the expected adhesive properties of the pad material can be calculated for species in the present study.

In the case of friction, the mechanical properties of a material may also contribute to the overall attachment force. The material of the fly pulvillus is soft; the membranous cuticle of setose pads is a fibrous composite material in which the fibres are not densely distributed. In Coleoptera, the setal bases are embedded in this material, providing high mobility of setae and thus adaptability to a variety of surface profiles (Beutel and Gorb, 2000). The setae or setal ends are also composed of an extremely flexible material. Among setose attachment systems, the flexible nature of setae has been demonstrated only for beetles, using Mallory's single stain (Stork, 1983), which stains tanned and untanned cuticle differently.

Scale effects on the surface microsculpture

Scale effects on the surface microsculpture have been reported previously in other insect attachment systems. The size and density of the seta-like hooks that couple the fore- and hindwing in Hymenoptera are dependent on animal size (Schneider and Schill, 1978). Scale effects have been reported for the microtrichia in different frictional devices of insects, such as the beetle elytra-to-body locking device (Gorb, 1998a) and fly armoured membranes (Gorb, 1997). In the beetle wing-locking device, a fivefold increase in body size results in an increase in both the length (up to fourfold), and the width (up to 2.3-fold) of microtrichia and a decrease in their density (up to fivefold). The dependence of the length and width of microtrichia on beetle size was linear, whereas that of microtrichial density was logarithmic. Among the fly species studied, the surface microsculpture (the area of the setal tip and setal density) varied significantly: larger flies have a lower setal density and larger setal tip areas. Therefore, the area of the setal tip correlated negatively with setal density.

Frictional properties of the pad material

The most interesting finding of this study is that the frictional properties of the material of the setal tips are not dependent on the dimensions of the fly species. In other words, frictional forces generated by the surface unit of the pulvillus are similar among the species studied (Fig. 10). The same result was obtained for the material of the setal tip (Fig. 11). Thus, the adhesive properties of the secretion and the mechanical properties of the setal tip material vary little, and differences in friction force must therefore mainly relate to

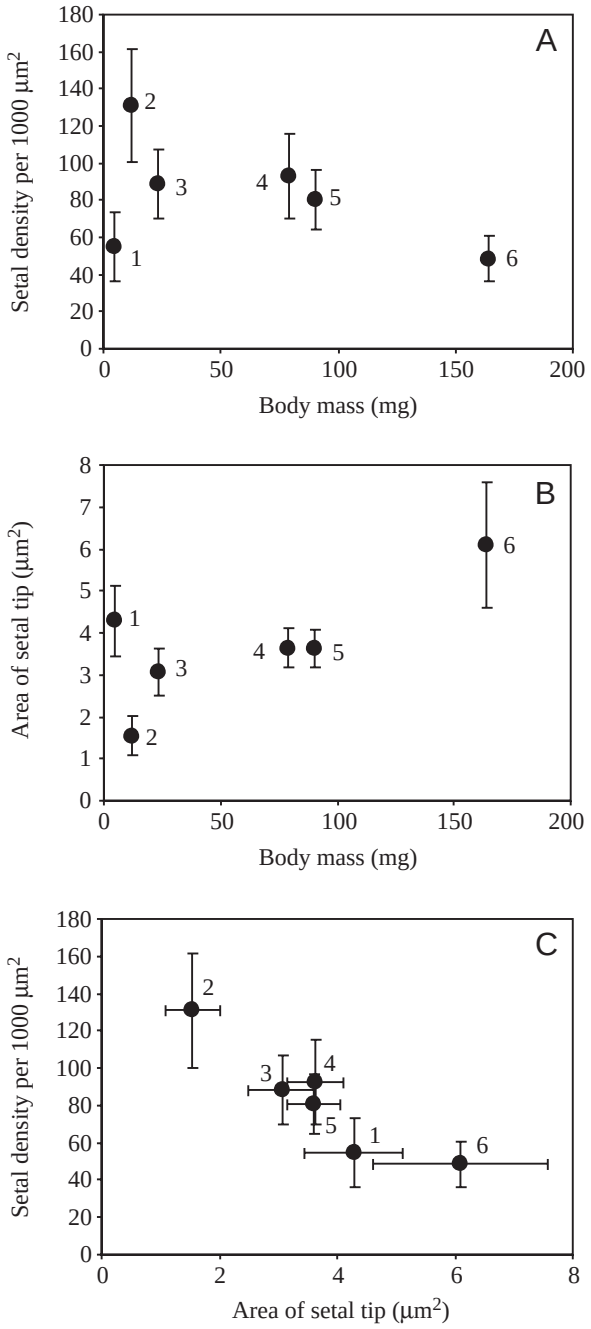

Fig. 9. (A) Setal density *D versus* body mass *m*. (B) Setal tip area S_1 *versus* body mass *m*. (C) Dependence of setal density *D* on the area of the setal tip S_1. Values are means ± S.D. (*n*=10 per species, *N*=3–11 depending on species, see Materials and methods). 1, *Platycheirus angustatus*; 2, *Sphaerophoria scripta*; 3, *Episyrphus balteatus*; 4, *Eristalis tenax*; 5, *Myathropa florea*; 6, *Volucella pellucens*.

variations in real contact area generated by the pad. Real contact area is the sum of the areas of the broadened setal tips of the pad in contact with the surface. Real contact area depends on the overall pad area, setal density and the area of a single setal tip. Although these variables vary among animals with different dimensions, the smaller setal tip area is

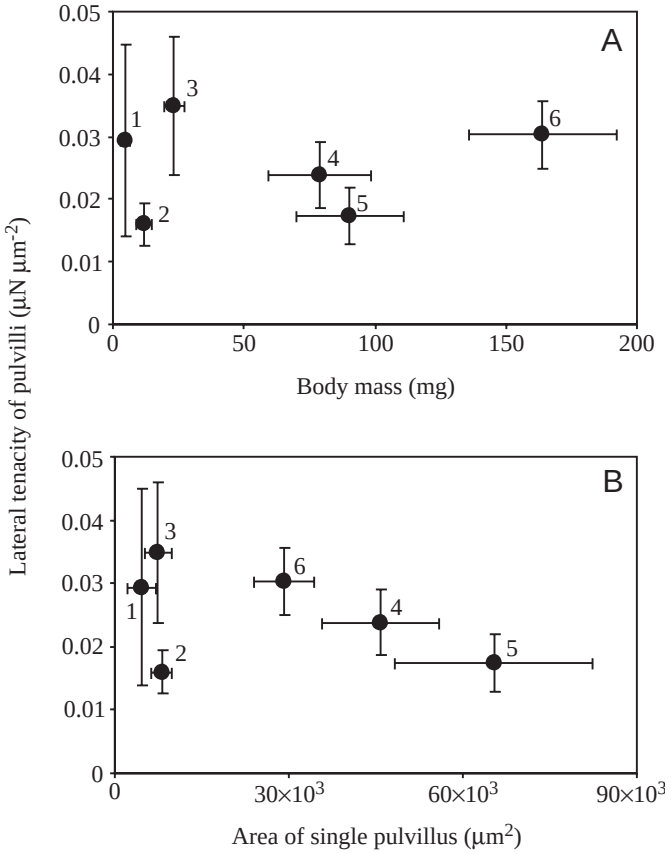

Fig. 10. Lateral tenacity of the fly pulvillus. (A) Lateral tenacity of the pulvillus τ_p *versus* body mass *m*. Linear regression: $\tau_p=0.025+6.351\times10^{-6}m$, F=0.01, P=0.923, one-way ANOVA. (B) Lateral tenacity τ_p *versus* pulvillus area S_1. Linear regression: $\tau_p=0.029-1.380\times10^{-6}S_1$, F=1.03, P=0.367, one-way ANOVA. Values are means ± S.D. (n=10 per species, N=3–11 depending on species, see Materials and methods). 1, *Platycheirus angustatus*; 2, *Sphaerophoria scripta*; 3, *Episyrphus balteatus*; 4, *Eristalis tenax*; 5, *Myathropa florea*; 6, *Volucella pellucens*.

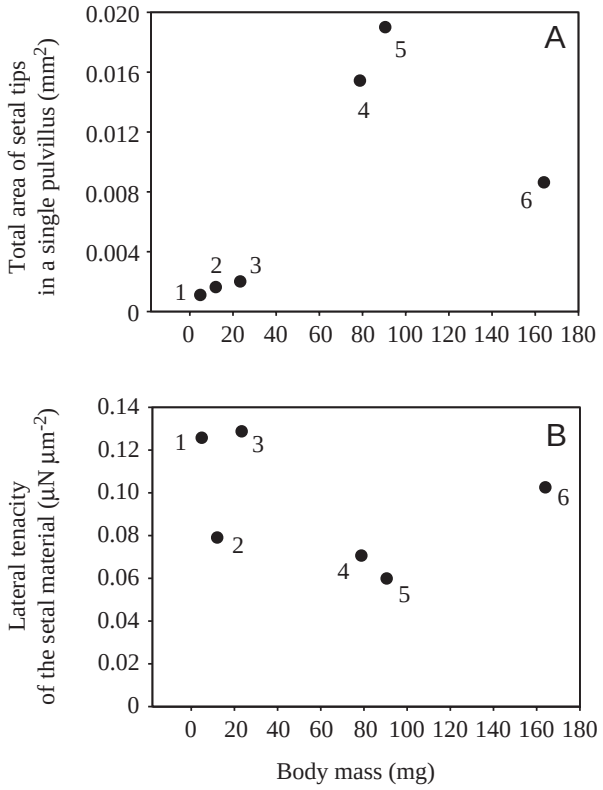

Fig. 11. (A) Real contact area S_r of all setae in a single pulvillus *versus* body mass *m*. Linear regression: $S_r=3.186+0.077m$, F=2.36, P=0.199, one-way ANOVA. (B) Lateral tenacity of the fly setae τ_m *versus* body mass *m*. Linear regression: $\tau_m=0.100-1.550\times10^{-4}m$, F=47.65, P=0.528, one-way ANOVA. (n=10 per species, N=3–11 depending on species, see Materials and methods). 1, *Platycheirus angustatus*; 2, *Sphaerophoria scripta*; 3, *Episyrphus balteatus*; 4, *Eristalis tenax*; 5, *Myathropa florea*; 6, *Volucella pellucens*.

compensated for by a higher setal density in the smaller species (Fig. 9C).

Scale effects on friction force

Although heavier species demonstrated higher friction forces (Fig. 4B), the ratio of friction force to body mass was significantly higher in the smallest species (*P. angustatus*: 36.16±18.12 mN mg^{-1}, N=6) compared with the largest species (*V. pellucens*: 6.29±1.56 mN mg^{-1}, N=5) (means ± S.D.; F=13.27, P=0.005, one-way ANOVA). The other four species had ratios intermediate between these two values. Friction force increases with an increase in pulvillus area (Figs 6B,D, 7B). However, the largest species does not have the largest pulvilli. Possibly, there are some design constraints on a further increase in the pad area. Since a twofold increase in pulvillus area results in a 1.5-fold increase in friction force (from 10 to 15 mN), it seems that a further increase in pulvillus area does not improve attachment ability. A possible explanation is that a further increase in pulvillus area could cause problems with the operation of a large attachment area so that a smaller number of setae would be able to make contact with the substratum. Data obtained from force measurements on a single hair of the gecko attachment pad support this suggestion: the attachment force of a single hair is greater than the force recalculated from measurements on a complete gecko foot (Autumn et al., 2000).

M. Mondon (Institute of Physics, University of Kaiserslautern, Germany) helped with contact angle measurements. Valuable discussions with Dr Y. Jiao, S. Niederegger (MPI of Developmental Biology, Tübingen, Germany), Dr M. Scherge (Ilmenau Technical University, Germany) and Dr W. Federle (Würzburg University, Germany) are greatly acknowledged. Two anonymous reviewers helped to improve an early version of the manuscript. TETRA GmbH (Ilmenau, Germany) contributed to the design of the centrifuge tester. This work is supported by the Federal Ministry of Education, Science and Technology, Germany, to S.G. (project BioFuture 0311851).

References

Autumn, K., Liang, Y. A., Hsieh, S. T., Zesch, W., Chan, W. P., Kenny, T. W., Fearing, R. and Full, R. J. (2000). Adhesive force of a single gecko foot-hair. *Nature* **405**, 681–685.

Bauchhenss, E. (1979). Die Pulvillen von *Calliphora erythrocephala* Meig. (Diptera, Brachycera) als Adhäsionsorgane. *Zoomorph.* **93**, 99–123.

Bauchhenss, E. and Renner, M. (1977). Pulvillus of *Calliphora erythrocephala* Meig. (Diptera; Calliphoridae). *Int. J. Insect Morph. Embryol.* **6**, 225–227.

Beutel, R. and Gorb, S. N. (2000). Evolution of tarsal and pretarsal attachment structures of insects (Arthropoda). *J. Zool. Systemat. Evol. Res.* (in press**)**.

Brainerd, E. L. (1994). Adhesion force of ants on smooth surfaces. *Am. Zool.* **34**, 128.

Dixon, A. F. G., Croghan, P. C. and Gowing, R. P. (1990). The mechanism by which aphids adhere to smooth surfaces. *J. Exp. Biol.* **152**, 243–253.

Dougherty, W. J. (1990). Barnacle adhesion: reattachment of the adult barnacle *Chthamalus fragilis* Darwin to polystyrene surfaces followed by centrifugational shearing. *J. Crust. Biol.* **10**, 469–478.

Edwards, J. S. and Tarkanian, M. (1970). The adhesive pads of Heteroptera: a re-examination. *Proc. R. Ent. Soc. Lond.* A **45**, 1–5.

Ernst, V. and Ruibal, R. (1967). The structure and development of the digital lamellae of lizards. *J. Morph.* **120**, 233–266.

Federle, W., Rohrseitz, K. and Hölldobler, B. (2000). Attachment forces of ants measured with a centrifuge: better 'wax-runners' have a poorer attachment to a smooth surface. *J. Exp. Biol.* **203**, 505–512.

Ghasi-Bayat, A. and Hasenfuss, I. (1980). Die Oberflächenstrukturen der Prätarsus von *Elasmucha ferrugata* (Fabricius) (Acanthosomatidae, Heteroptera). *Zool. Anz.* **205**, 76–80.

Gillett, J. D. and Wigglesworth, V. B. (1932). The climbing organ of an insect, *Rhodnius prolixus* (Hemiptera, Reduviidae). *Proc. R. Soc. Lond. B* **111**, 364–376.

Gorb, S. N. (1997). Armored cuticular membranes in Brachycera (Insecta, Diptera). *J. Morph.* **234**, 213–222.

Gorb, S. N. (1998a). Frictional surfaces of the elytra to body arresting mechanism in tenebrionid beetles (Coleoptera: Tenebrionidae): design of co-opted fields of microtrichia and cuticle ultrastructure. *Int. J. Insect Morph. Embryol.* **27**, 205–225.

Gorb, S. N. (1998b). The design of the fly adhesive pad: distal tenent setae are adapted to the delivery of an adhesive secretion. *Proc. R. Soc. Lond. B* **265**, 747–752.

Gorb, S. N., Jiao, Y. and Scherge, M. (2000). Ultrastructural architecture and mechanical properties of attachment pads in *Tettigonia viridissima* (Orthoptera Tettigoniidae). *J. Comp. Physiol.* A **186**, 821–831.

Hasenfuss, I. (1977). Die Herkunft der Adhäsionsflüssigkeit bei Insekten. *Zoomorph.* **87**, 51–64.

Hasenfuss, I. (1978). Über das Haften von Insekten an glatten Flächen – Herkunft der Adhäsionsflüssigkeit. *Zool. Jb. Anat.* **99**, 115–116.

Highley, K., Coomey, M., Denbeste, M. and Wolfram, L. (1977). Frictional properties of skin. *J. Invest. Dermatol.* **69**, 303–305.

Irschick, D. J., Austin, C. C., Petren, K., Fisher, R. N., Losos, J. B. and Ellers, O. (1996). A comparative analysis of clinging ability among pad-bearing lizards. *Biol. J. Linn. Soc.* **59**, 21–35.

Ishii, S. (1987). Adhesion of a leaf feeding ladybird *Epilachna vigintioctomaculata* (Coleoptera: Coccinellidae) on a vertically smooth surface. *Appl. Ent. Zool.* **22**, 222–228.

Jiao, Y., Gorb, S. N. and Scherge, M. (2000). Adhesion measured on the attachment pads of *Tettigonia viridissima* (Orthoptera, Insecta). *J. Exp. Biol.* **203**, 1887–1895.

Lees, A. M. and Hardie, J. (1988). The organs of adhesion in the aphid *Megoura viciae*. *J. Exp. Biol.* **136**, 209–228.

Persson, B. N. J. (1998). *Sliding Friction. Physical Principles and Applications*. Berlin, Heidelberg, New York: Springer.

Podczeck, F. and Newton, J. (1995). Development of an ultracentrifuge technique to determine the adhesion and friction properties between particles and surfaces. *J. Pharmac. Sci.* **84**, 1067–1071.

Rabinowicz, E. (1995). *Friction and Wear of Materials*. New York: Wiley.

Richards, P. A. and Richards, A. G. (1969). Acanthae: a new type of cuticular process in the proventriculus of Mecoptera and Siphonaptera. *Zool. Jb. Anat.* **86**, 158–176.

Röder, G. (1984). Morphologische Untersuchungen an Prätarsen von Diptera and Mecoptera (Insecta). Dissertation, Universitä Nürnberg.

Roth, L. M. and Willis, E. R. (1952). Tarsal structure and climbing ability of cockroaches. *J. Exp. Biol.* **119**, 483–517.

Ruibal, R. and Ernst, V. (1965). The structure of the digital setae in lizards. *J. Morph.* **117**, 271–294.

Schneider, P. and Schill, R. (1978). Der Gleitkoppelmechanismus bei vierflügeligen Insekten mit asynchronem Flugmotor. *Zool. Jb. Physiol.* **82**, 365–382.

Stork, N. E. (1980a). A scanning electron microscope study of tarsal adhesive setae in the Coleoptera. *Zool. J. Linn. Soc.* **68**, 173–306.

Stork, N. E. (1980b). Experimental analysis of adhesion of *Chrysolina polita* (Chrysomelidae, Coleoptera) on a variety of surfaces. *J. Exp. Biol.* **88**, 91–107.

Stork, N. E. (1983). The adherence of beetle tarsal setae to glass. *J. Nat. Hist.* **17**, 583–597.

Walker, G., Yule, A. B. and Ratcliffe, J. (1985). The adhesive organ of the blowfly, *Calliphora vomitoria*: a functional approach (Diptera: Calliphoridae). *J. Zool., Lond.* **205**, 297–307.